

## GAUSSIAN FILTER FOR BRAIN SPECT IMAGING

N.A. Nikolov<sup>1,4\*</sup>, S.S. Makeev<sup>2</sup>, O. Korostynska<sup>3</sup>, T.G. Novikova<sup>2</sup>, Ye.S. Kriukova<sup>1</sup>

<sup>1</sup>Igor Sikorsky Kyiv Polytechnic Institute, Kyiv, Ukraine

<sup>2</sup>Romodanov Neurosurgery Institute, NAMS of Ukraine, Kyiv, Ukraine

<sup>3</sup>Oslo Metropolitan University, Oslo, Norway

<sup>4</sup>Kundiiev Institute of Occupational Health, NAMS of Ukraine, Kyiv, Ukraine

\*Corresponding author: nikolka\_@ukr.net

Received 7 January 2022; Accepted 2 February 2022

**Background.** The presence of a noise component on 3D images of single-photon emission computed tomography (SPECT) of a brain significantly distorts the probability distribution function (PD) of the radioactive count rate in the images. The presence of noise and further filtering of the data, based on a subjective assessment of image quality, have a significant impact on the calculation of volumetric cerebral blood flow and the values of the uptake asymmetry of the radiopharmaceutical in a brain.

**Objective.** We are aimed to develop a method for optimal SPECT filtering of brain images with lipophilic radiopharmaceuticals, based on a Gaussian filter (GF), for subsequent image segmentation by the threshold method.

**Methods.** SPECT images of the water phantom and the brain of patients with <sup>99m</sup>Tc-HMPAO were used. We have developed a technique for artificial addition of speckle noise to conditionally flawless data in order to determine the optimal parameters for smoothing SPECT, based on a GF. The quantitative criterion for optimal smoothing was the standard deviation between the PD of radioactive count rate of the smoothed image and conditionally ideal one.

**Results.** It was shown that the maximum radioactive count rate of the SPECT image has an extremum by changing the standard deviation of the GF in the range of 0.3–0.4 pixels. The greater the noise component in the SPECT image, the more quasi-linearly the corresponding rate changes. This dependence allows determining the optimal smoothing parameters. The application of the developed smoothing technique allows restoring the probability distribution function of the radioactive count rate (distribution histogram) with an accuracy up to 5–10%. This provides the possibility to standardize SPECT images of brain.

**Conclusions.** The research results of work solve a specific applied problem: restoration of the histogram of a radiopharmaceuticals distribution in a brain for correct quantitative assessment of regional cerebral blood flow. In contrast to the well-known publications on the filtration of SPECT data, the work takes into account that the initial tomographic data are 3D, rather than 2D slices, and contain not only uniform random Gaussian noise, but also a pronounced speckle component.

**Keywords:** emission computed tomography; SPECT; cerebral blood flow; radioactive count; Gaussian filter; optimal filtering; speckle-noise; radiopharmaceutical; <sup>99m</sup>Tc-HMPAO.

### Introduction

The main objective of scintigraphic studies of brain with lipophilic radiopharmaceuticals is the studying brain efficient perfusion. In this regard, a method for quantitative assessment of absolute volume of cerebral blood flow (CBF) was developed [1, 2]. The term "absolute" implies the calculation of CBF without reference to any segment of the brain with known parameters of effective perfusion, for example, using the well-known Lassen's method [3, 4]. Methodology and software for the calculation of the CBF, developed by our working group, make it possible to measure absolute values of volumetric blood flow directly. The accumulated clinical experience of calculation usage of the abso-

lute CBF method [1, 2] and the development of appropriate software were resulted in a set of data analysis features [5].

The method is based on the fact that a brain is represented as a flow system. In accordance with the proposed model, a fluid with a volume velocity  $v$  and a material with a concentration of  $z$  dissolve flow to the container of volume  $V$  with ideal instant mixing. A part of the material is specifically captured by perceiving surface elements, another part is removed from the tank. However, the effective volume of radiopharmaceutical dilution in blood  $V$  is not equal to the volume of the brain ( $V_0$ ), but represents a certain effective value ( $V < V_0$ ). The corresponding empirical dependence was obtained for determining the effective volume of radiopharmaceuticals dilu-

tion in brain based on regression and statistical analysis. Based on this dependence, the threshold for segmentation of single-photon emission computed tomography (SPECT) data was determined. The amount of voxels exceeds this threshold and is the desired volume. Based on this method, clinical data were obtained and their adequacy was indicated. However, sometimes quantitative values of blood flow inadequate to physiologically accepted values were observed. The detailed analysis of such cases showed that the main error of the calculations was associated with the degree of smoothing SPECT images of the brain. The brain segmentation threshold for determining the volume  $V$  is calculated from the maximum accumulation of the radiopharmaceutical in a brain. A similar approach was used, in particular, in analysis of brain by SPECT in the diagnosis of Alzheimer's disease [6]. It should also be noted that the quality of radionuclide images is limited not only by hardware capabilities, but also by the number of radiopharmaceuticals administered to the patient and the functional state of other organs and systems [7–9]. There are a significant shift of the histogram of velocity distribution of radioactive count rate (CR) and a change in the maximum CR in smoothing SPECT. Due to the high level of noise in SPECT images and low brain perfusion, extremely low values of CBF were observed; at a sufficiently high accumulation of the radiopharmaceutical in a brain, even minor smoothing led to inappropriately large values of CBF. In this regard, the task was to determine the optimal degree of smoothing of SPECT data. By optimal smoothing, we mean the minimal 3D smoothing (filtering) of an image, which makes it possible to bring the histogram (probability distribution function) of the radiopharmaceutical distribution in a brain to the conditionally necessary one in order to obtain adequate values of  $V$ . At the same time, this filtering should not impair perception of images at a qualitative visual level.

In this case, the criteria for assessing the quality of filtering are the subjective visual assessment of the image quality and the smallest Root Mean Square Error (RMSE) of CR of the results for some conditionally ideal image [10]. In the last case, the conditionally ideal SPECT image is obtained when conducting a study with a long exposure time of one projection frame.

Based on the analysis of scientific literature and our own experience in researching methods for determining the optimal filtering of SPECT images, we can point out the following methodological errors and incorrect experimental design:

- images are often represented by regions with a uniform distribution of brightness, while scintigraphic images, especially of patients, are always gradient in computer modeling;
- incorrect artificial data noise;
- one SPECT image requires approximately 20–40 min, when carrying out phantom scintigraphic studies, which does not allow obtaining a sufficient amount of data of different quality under equivalent conditions, since radioactive decay occurs, CR changes, the signal-to-noise ratio changes;
- in most cases, a small number of patient images are analyzed;
- it is not taken into account that the textural properties of SPECT can differ significantly from the norm in case of pathologies [11].

As a result, the issue related to the optimal filtering of medical images in a specific SPECT brain has not been completely resolved [12]. In addition, the optimal filtering parameters depend on the purpose and objectives of image analysis. For example, visualization of images, their segmentation, quantitative and texture analysis may require different approaches.

The aim of this work is to develop a method for optimal SPECT filtering of brain images with lipophilic radiopharmaceuticals based on a Gaussian filter for subsequent image segmentation by the threshold method.

## Methods

The study has used SPECT images of the water phantom and 20 patients with different levels of brain perfusion, the change in the texture properties of SPECT images depended on the filtering parameters.

The water phantom was a cylinder 20 cm in diameter and 40 cm high. The exposure time of one frame during studies with  $^{99m}\text{Tc}$ -pertechnetate was 20 s, 15 s, 10 s, 5 s; data collection matrix – 64×64 and 128×128, the activity – 50 MBq. To ensure uniform distribution of  $^{99m}\text{Tc}$ -pertechnetate in the phantom, the initial amount of water in it was about 2/3 of the total volume. This allows shaking and ensures good mixing. After that, the phantom was completely filled with water and settled for about 20 min. The uniformity of radioactivity distribution in the water phantom was monitored on planar (2D) scintigraphic images. The correction for gamma radiation absorption has not been taken into account during the reconstruction of SPECT for obtaining an uneven texture of the phantom SPECT image, which is more similar to the distribution of the radiopharmaceutical in a brain.

Patients were examined using  $^{99m}\text{Tc}$ -hexamethylpropyleneamine oxime ( $^{99m}\text{Tc}$ -HMPAO). SPECT was carried out 15–20 min after intravenous administration of the radiopharmaceutical. The tomographic study included the collection of 64 projections for the matrix of  $64 \times 64$  or 128 projections for the matrix of  $128 \times 128$ , the activity of the radiopharmaceutical when administered intravenously was 740 MBq.

Scintigraphic data were obtained on a gamma camera "E. Cam" (Siemens) equipped with a LEHR collimator.

Image processing and analysis were carried out in the Matlab 2018 environment in the application "ScintyBrain" with the user interface developed by the authors [5].

The obtained SPECT images were smoothed by a Gaussian filter with the filter order  $[n_x, n_y, n_z]$  and standard deviation  $[\sigma_x, \sigma_y, \sigma_z]$ ;  $n_x = n_y = n_z = n_f$ ;  $\sigma_x = \sigma_y = \sigma_z = \sigma_f$ .  $n_f$  took the values 3, 5, 7 and 9;  $\sigma_f$  – from 0.1 to 7 in increments of 0.1. The optimal smoothing parameters  $n_{f0}$  and  $\sigma_{f0}$  were chosen by minimum RMSE between the probability distribution functions (PD) of CR ( $p = f(Q)$ ) of smoothed SPECT images and conditionally ideal one. As theoretically ideal distribution functions, we considered the distribution of the SPECT image matrix of  $128 \times 128$  with an exposure time of one frame of 20 s.

SPECT images, selected by expert-qualitative visual level, belonged to conditionally ideal PD of CR in patients. All patients had the CBF of the brain hemisphere either within normal limits or increased, which corresponded to a percentage of radiopharmaceutical penetration into the brain of more than 3% of the administered activity. Also, to minimize the influence of digital noise, the ideal SPECT images were smoothed by a Gaussian filter with  $n_f = 3$ ,  $\sigma_f = 0.3$ . These are the minimum values at which the minimal visual effect of smoothing is observed. Based on the results of SPECT smoothing, we have compared images obtained at different resolutions and exposure times of one frame during the preliminary study. However, due to the duration of SPECT, it is impossible to record a sufficiently large amount of data under equivalent conditions for statistical and regression analysis. So, an algorithm for noise reduction of conditional ideal images was developed. The use of this algorithm made it possible to vary the SPECT image quality over a wide range and to estimate the optimal filter parameters. The noise distribution was estimated by the difference between the conditionally ideal images and SPECT obtained with shorter frame exposure time for phantom images. Graphical results of this analysis are presented in Fig. 1, where  $Q_n$  – CR normalized by the maximum velocity in the whole 3D SPECT image ( $Q_{\max}$ ).

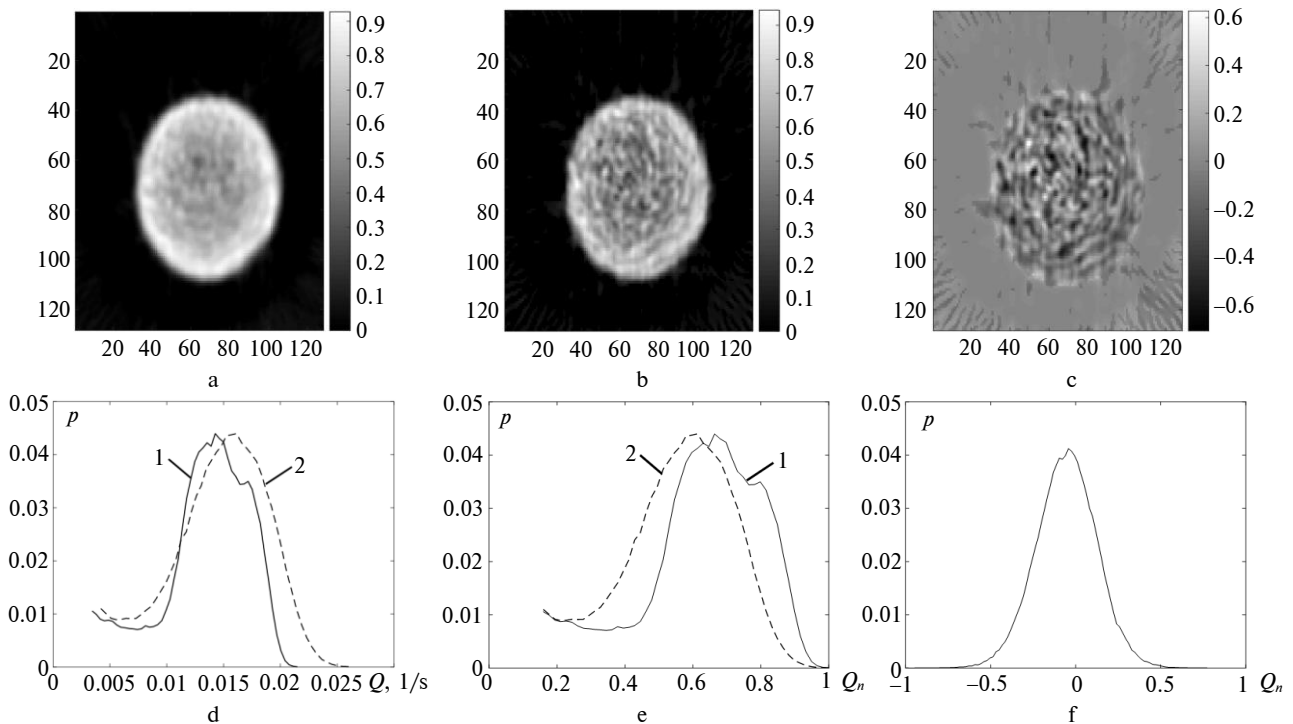


**Figure 1:** Evaluation of the spatial distribution of SPECT noise: (a), (b) transverse slices normalized to the maximum radioactivity of the phantom image obtained at the exposure times of the projection frame: (a) 20 s, (b) 10 s; (c) differential SPECT image obtained under conditions (a) and (b); (d), (e) probability distribution function of 3D SPECT images for an exposure time of 20 s – 1, 10 s – 2; (f) is a noise probability distribution function of the 3D difference image (c)

The analysis of the data in Fig. 1 shows the following. With the decrease in the exposure time of projection images,  $Q_{\max}$  can differ significantly (by more than 5–10%) from the conditionally true value in the reconstructed 3D image (Fig. 1d). This causes the histogram or  $p = f(Q)$  to shift to the right. As a result, the presence of the noise component shifts  $p = f(Q_n)$  towards lower values of the radioactive CR after SPECT normalization to  $Q_{\max}$ , i.e. to the left (Fig. 1e).  $p = f(Q_n)$  for the SPECT differential image; one of the sections shown in Fig. 1c shows the normal Gaussian noise distribution (Fig. 1f). This is one of the main features that led to the study of the possibilities of using Gaussian smoothing in this work.

However, Fig. 1c indicates that the noise component in SPECT images is represented by speckle noise in the useful region (phantom region); thus, the farther the phantom is from the center (the axis of the gamma-camera detector rotation), the more the speckle patterns are extended radially. In addition, it is noteworthy that the spatial distribution of artifacts is qualitatively different in the useful region and in the background one. Speckles associated with the effects of a "star" (or "streak") artifact dominate in the background region [13]. In this regard, the optimal filtering (smoothing) parameters should be different for the useful SPECT region and the background one. In this work, we study the optimal filtering for a useful region, i.e. phantom or brain regions. The threshold method was used to separate the useful region from the background: the one where  $Q(x, y, z) > 0.15 Q_{\max}$  was considered a useful region. This also allows minimizing the influence of the background on  $p = f(Q)$  and the subsequent estimation of the standard deviation of the smoothed images from conditionally ideal ones, since the volume of the background region is quite large and can exceed the useful region.

The latter feature has not been emphasized in the literature. It should also be noted that the threshold of  $0.15 Q_{\max}$  adequately separates the phantom image from the background, since the boundary is clear, while for brain images this value is ambiguous due to the uneven distribution of the radiopharmaceuticals. This complicates an unambiguous assessment of the smoothing effect of brain SPECT. However, this feature did not affect the general results of this work.

Thus, the SPECT image noise reduction algorithm mentioned above is a speckle noise generation technique whose probability distribution function obeys the Gaussian distribution:

$$G(x, y, z) = M \cdot \exp \left\{ - \left( \frac{(x - x_0)^2}{2\sigma_{x\text{nois}}^2} + \frac{(y - y_0)^2}{2\sigma_{y\text{nois}}^2} + \frac{(z - z_0)^2}{2\sigma_{z\text{nois}}^2} \right) \right\}, \quad (1)$$

where  $G(x, y, z)$  is the Gaussian distribution of an individual speckle-noise pattern,  $x_0, y_0, z_0$  are coordinates of the pattern,  $\sigma_{x\text{nois}}, \sigma_{y\text{nois}}, \sigma_{z\text{nois}}$  are standard deviations,  $M$  is an intensity of the pattern.

The speckle-noise generation algorithm for SPECT image is reduced to the following steps:

1. Downloading the original SPECT image ( $I_0$ ) and the formation of the 3D zero matrix ( $I_g$ ), size  $I_0$ .
2. Setting the noise parameters: maximum intensity ( $M_0$ );  $\sigma_{x\text{nois}}, \sigma_{y\text{nois}}, \sigma_{z\text{nois}}$ ; the minimum geometric size of the Gaussian speckle-noise pattern  $d_x, d_y, d_z$ ; number of iterations, i.e. the number of patterns ( $n$ ); the angle  $\alpha$  in the  $xy$  plane with respect to the centre of detector rotation, at which the pattern will be blurred.
3. Specifying the region of noise ( $\Omega$ ). In this paper, the useful volume was separated from the background region based on the threshold segmentation  $I_0$ .  $\Omega$  is the region where  $I_0$  assumed values of more than a given level ( $Th$ ) from the maximum radioactive CR  $Q_{\max}$ .
4. Generation according to the uniform distribution law of random coordinates  $(x_0, y_0, z_0) \in \Omega$  and noise intensity ( $M$ ) according to the normal distribution law that limits the values of  $M_0$  ( $M \in [-M_0, +M_0]$ ).
5. The formation of the Gaussian speckle noise pattern in the  $I_g$  image according to the equation (1), where  $x \in [x_0 - d_x/2, x_0 + d_x/2]$ ,  $y \in [y_0 - d_y/2, y_0 + d_y/2]$ ,  $z \in [z_0 - d_z/2, z_0 + d_z/2]$ .
6. Transferring/stretching the pattern formed in the previous step by the angle  $\alpha$  parallel to the  $xy$  plane.
7. Repeating  $n$  times for steps 4–6.
8. SPECT image formation of  $I_{Gn}$  with Gaussian speckle noise by summing  $I_g$  and  $I_0$  and zeroing the obtained negative values.

The following assumptions were made for SPECT with the matrix of  $128 \times 128$  by implementing the above algorithm:  $\sigma_x = \sigma_y = \sigma = 1.5$ ;  $\sigma_z = \sigma/2$ ;  $d = d_x = d_y = d_z$  (for the data acquisition matrix of  $64 \times 64$ :  $d = 3$ ,  $128 \times 128$ :  $d = 5$ ,  $256 \times 256$ :  $d = 7$ );  $\alpha = 26^\circ$ ,  $Th = 0,15$ . The number of iterations is  $n = 12000$ . Thus, the noise level of the  $I_{Gn}$  image and the distortion of the histogram of the CR distribution were determined by the parameter  $M_0$  for the indicated parameter values.

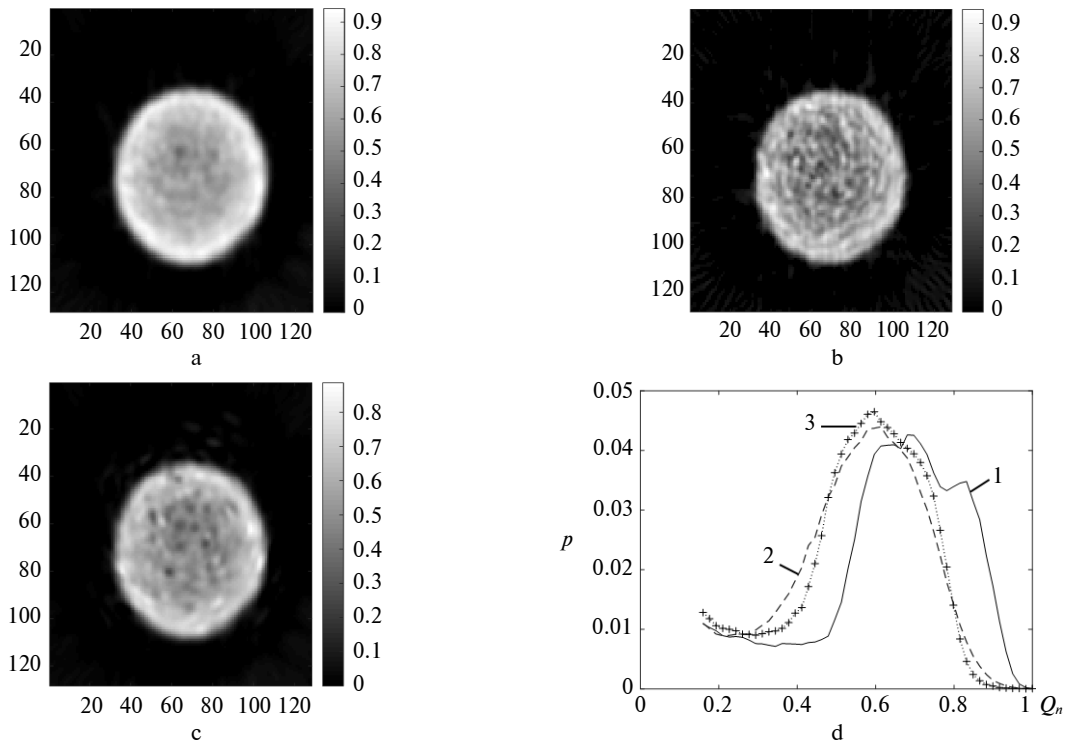


**Figure 2:** Cross-section of a water phantom. An example of the SPECT distortion by speckle noise: (a), (b) initial phantom cross-sections obtained at exposure times of one frame of 20 s (a) and 10 s (b); (c) the result of adding speckle noise to image (a); (d) the probability distribution function of the normalized radioactive count rate: 1 – SPECT with a projection frame exposure time of 20 s, 2 – 10 s, 3 – after adding speckle noise

## Results

Fig. 2 shows the results of artificial noise in SPECT images of a water phantom based on the developed algorithm. Histogram analysis of the corresponding 3D images indicates a fairly adequate coincidence  $p = f(Q_n)$  of the artificially noisy image and SPECT (curves 3 and 2 respectively in Fig. 2g), which was obtained with a reduced exposure time of the projection frame during data collection.

Fig. 3 shows the result of changing the function  $p = f(Q_n)$  depending on the maximum speckle-noise intensity ( $M_0$ ) (see (1) and Section 4 in the noise generation algorithm in the previous subsection). As  $M_0$  increases, the maximum probability of the normalized radioactive CR  $Q_n$  increases its value and shifts toward lower  $Q_n$  values; with increasing  $M_0$ , the general form  $p = f(Q_n)$  qualitatively retains its shape, however, some smoothing of the characteristic irregularities of the conditionally ideal curve is observed (curve  $M_{00}$  in Fig. 3). The heterogeneity data has been restored after the optimal filtering procedure.

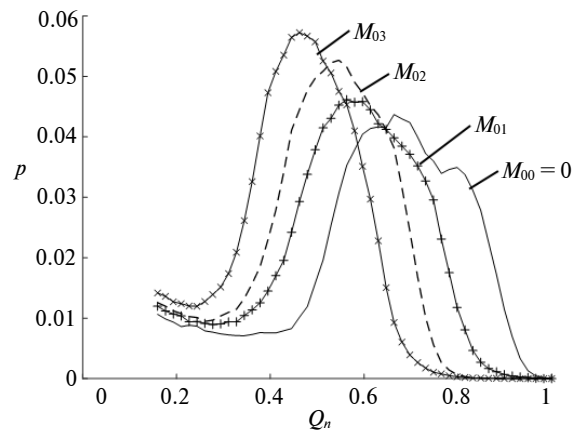


**Figure 3:** Change in the function  $p = f(Q_n)$  depending on the maximum intensity of speckle noise ( $M_0$ ):  $M_{00} = 0$  – absence of artificial noise;  $M_{01} < M_{02} < M_{03}$

The change in RMSE between the  $p = f(Q_n)$  of the conditionally ideal SPECT of the water phantom and the artificially noisy image, as well as the change in the maximum ( $Q_{n\max}$ ) and average brightness ( $Q_{n\text{mean}}$ ) after subsequent smoothing by a 3D Gaussian filter with different values of  $\sigma_f$  and  $n_f$  are

presented in Fig. 4. Graphical dependencies show a monotonic decrease in  $Q_{n \max}$  and  $Q_{n \text{mean}}$  with increasing  $\sigma_f$  and  $n_f$  (Fig. 4a,b). Moreover the average value changed by no more than 11% (the range of change  $Q_{n \text{mean}} \approx 0.42\text{--}0.47$ ) after sufficiently strong SPECT smoothing, while the maximum value of  $Q_{n \max}$  (Fig. 4b) shows a rather high sensitivity to the parameters of the smoothing function (the range of change  $Q_{n \max} \approx 0.7\text{--}1$ ,  $Q_{n \max} = 1$  matches the image without smoothing).

When speckle noise is added to the conditionally ideal SPECT phantom image, the subsequent smoothing of the 3D image of the RMSE of the functions  $p = f(Q_n)$  of the initial and smoothed images with increasing  $\sigma_f$  is characterized by the presence of a minimum point (Fig. 4c, curves  $n_f = 7$  and 9). The dependencies presented in Fig. 4 correspond to sufficiently strong SPECT noise, where  $p = f(Q_n)$  is shown in Fig. 3 for  $M_{03}$ . In this case, smoothing SPECT by a Gaussian filter with the order  $n_f = 3$  and 5 does not lead to the formation of extreme curves.

The rate of change  $Q_{n \max}$  was estimated based on the approximation depending on  $\sigma_f$ :

$$\Delta Q_{n \max} / \Delta \sigma_f = \frac{Q_{n \max}(\sigma_f + \Delta \sigma_f) - Q_{n \max}(\sigma_f)}{\Delta \sigma_f}.$$

The examples of graphical dependencies of changes in  $\Delta Q_{n \max} / \Delta \sigma_f$  for various values  $\sigma_f$  and  $n_f$  are presented in Fig. 5. The maximum of  $|\Delta Q_{n \max} / \Delta \sigma_f|$  for phantom was observed for  $\sigma_f = 0.3\text{--}0.4$ , regardless of the noise level and  $n_f$  (Fig. 5a). The presence of the noise component on SPECT affects the absolute value of  $\Delta Q_{n \max} / \Delta \sigma_f$  (Fig. 5b): an increase in the noise parameter  $M_0$  leads to sharper drops  $\Delta Q_{n \max} / \Delta \sigma_f$  in the vicinity of  $\sigma_f = 0.3\text{--}0.4$ .

The regression analysis of the optimal values of  $\sigma_{f0}$  and  $n_{f0}$  at various levels of SPECT speckle-noise intensity showed that the section of the curve  $\Delta Q_{n \max} / \Delta \sigma_f$  at  $\sigma_f = 0.05\text{--}0.4$  is quasi-linear, the slope of which characterizes the optimal value of  $\sigma_{f0}$  with sufficient accuracy (Fig. 6a). In Fig. 6, the  $D_Q$  is value of  $\Delta Q_{n \max} / \Delta \sigma_f$  at  $\sigma_f = 0.3$ . The optimal para-

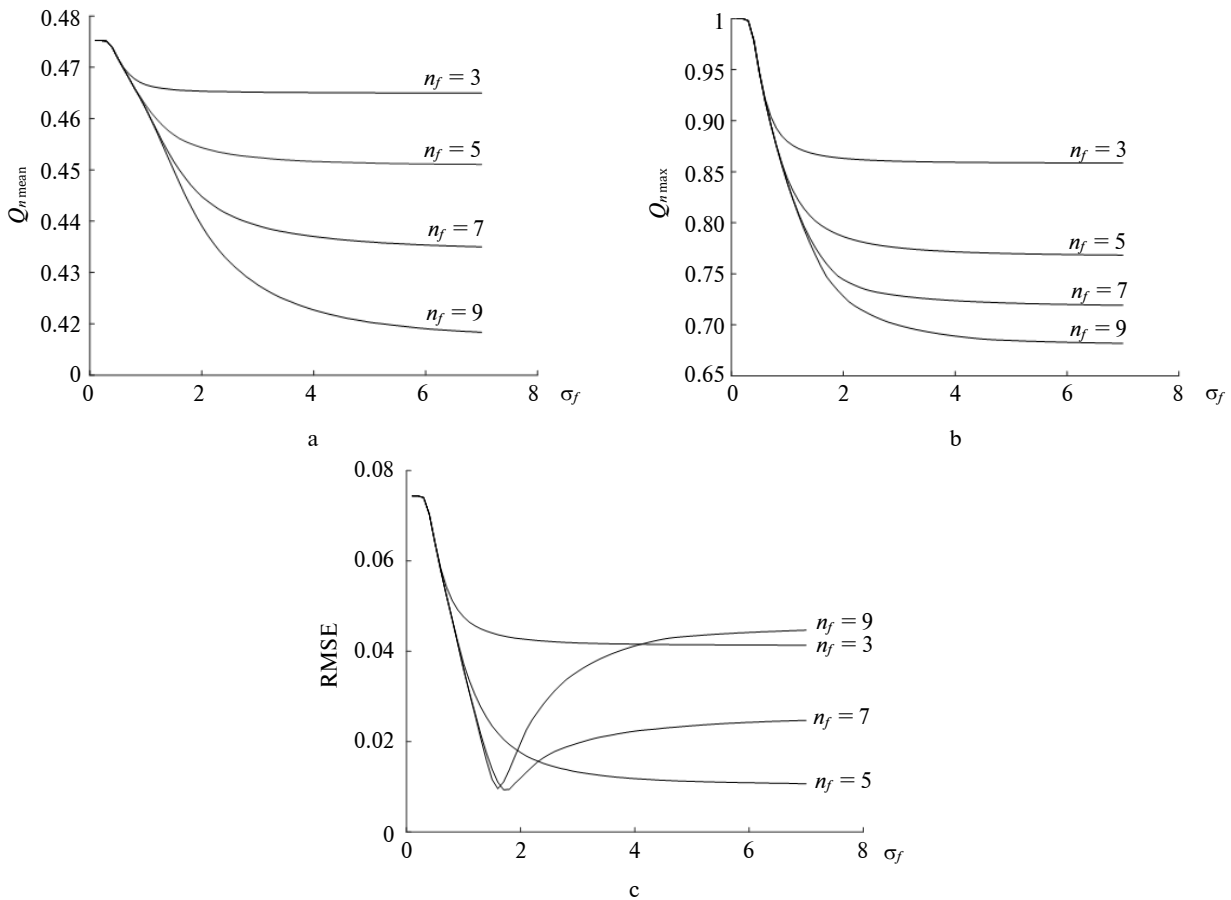


**Figure 4:** Change of the textural properties of the water phantom SPECT at various Gaussian smoothing parameters: (a) average count rate; (b) maximum count rate; (c) Root Mean Square Error between  $p = f(Q_n)$  for the conditionally ideal image and smoothing image with noise

eters  $\sigma_{f0}$  and  $n_{f0}$  can generally show some independence from each other. However, it is possible to require and impose the condition of the direct dependence of the increase in  $n_{f0}$  on  $\sigma_{f0}$  (Fig. 6b).

Water phantom studies have also been presented on SPECT patients. In these cases, all the patterns presented in this work were equivalent to phantom studies, which is confirmed by the regression data in Fig. 6. The resulting regression equations were as follows:

for SPECT patients

$$\sigma_{f0} = -(6.57 \pm 1.3)D_{Q0.4} + (0.20 \pm 0.11) \quad (R^2 = 0.75 \pm 0.31),$$

$$n_{f0} = (1.46 \pm 0.7)\sigma_{f0} + (2.57 \pm 0.27) \quad (R^2 = 0.62 \pm 0.11);$$

for phantom SPECT

$$\sigma_{f0} = -(6.5 \pm 0.3)D_{Q0.4} + (0.16 \pm 0.10) \quad (R^2 = 0.81 \pm 0.05),$$

$$n_{f0} = (1.92 \pm 0.05)\sigma_{f0} + (2.42 \pm 0.14) \quad (R^2 = 0.79 \pm 0.04),$$

where  $R$  is the correlation coefficient between the experimental and model data.

We recommend to apply smoothing with minimally significant parameters for 3D images  $\sigma_f = 0.3$  and  $n_f = 3$ , because real SPECT images always have a noise component, including digital noise, even with good image quality (see Fig. 5b at  $M_{00}$ ). The recommended values for optimal SPECT filtering can be expressed as:

$$\sigma_{f0} = -6,57D_{Q0.4} + 0.2 \text{ and } n_{f0} = 1.1\sigma_{f0} + 3, \quad (3)$$

where  $n_{f0}$  is rounded up to the nearest of 3, 5, 7, or 9.

A cumulative use of (2) to calculate the most effective smoothing parameters of the 3D SPECT Gaussian filter both for phantom images and patients gives a fairly good agreement of the functions  $p = f(Q_n)$ , where the average deviation of the CR is less than 5–7%, the maximum deviation is observed in the low-intensity region ( $Q_n < 0.5$ ), where the error in the restoring the function  $p = f(Q_n)$  reaches 10–12%. The used examples (2) are presented in Figs. 7 and 8. Note that when segmenting the brain and determining the effective volume of dilution of the radiopharmaceutical in accordance with the methodology for calculating CBF [1, 2, 5], the segmentation threshold  $Th$  is in the range 0.55–0.90. This means that the results of finding the optimal parameters  $\sigma_{f0}$  and  $n_{f0}$  for a Gaussian filter are quite acceptable.

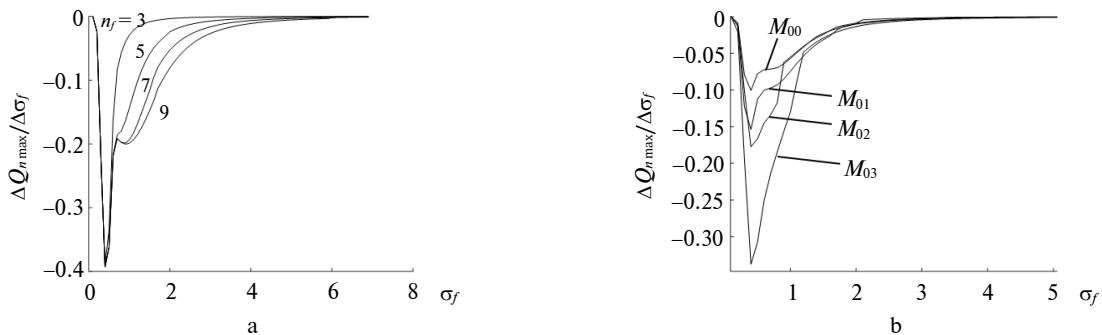


**Figure 5:** The rate of change count range with respect to  $\sigma_f$ : (a) for SPECT of the water phantom at  $M_{03}$ ; (b) for various of  $M_0$ . The effect of  $M_{0i}$  on  $p = f(Q_n)$  (see Fig. 3). The order of the Gaussian filter  $n_f$  does not affect the extremum in the vicinity of  $\sigma_f = 0.3$ –0.4

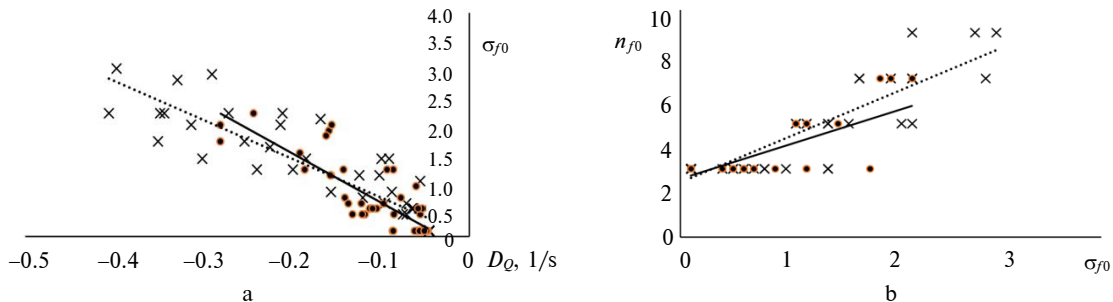


**Figure 6:** Regression dependencies of the optimal parameters  $\sigma_{f0}$  and  $n_{f0}$  obtained at different speckle noise intensities on SPECT: (a) the dependence of  $\sigma_{f0}$  on  $D_Q$ ; (b) the dependence of  $n_{f0}$  on  $\sigma_{f0}$ ;  $\times$  – for SPECT water phantom;  $-$  – for SPECT of the patient; the dashed line is a linear approximation of the SPECT data of the water phantom, the solid line is for the SPECT of the patient

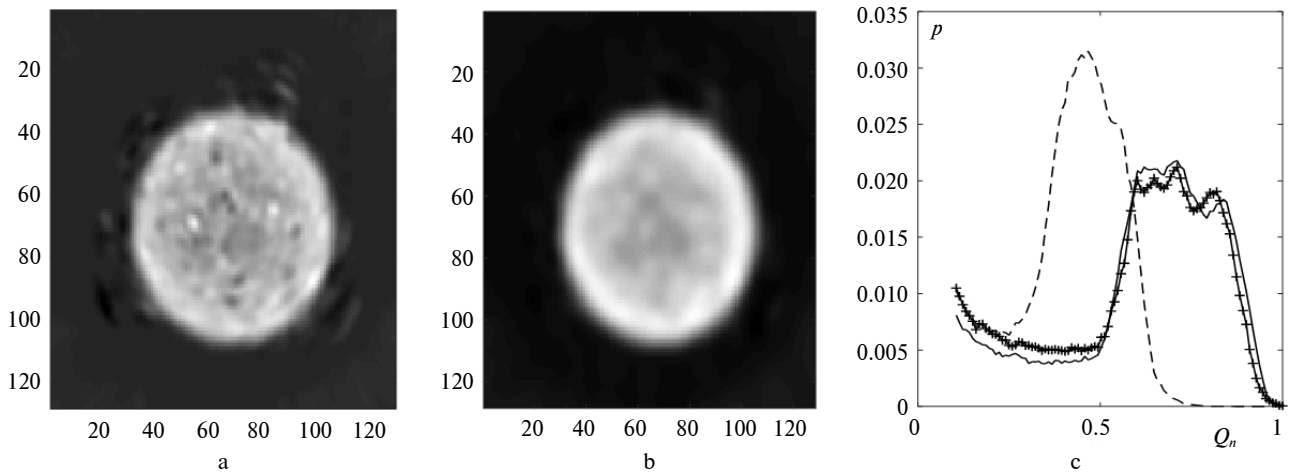


**Figure 7:** The results of smoothing SPECT of the water phantom in accordance with (2): (a), (b) cross-sections of the phantom after adding speckle noise and smoothing, respectively; (c) the probability distribution function of the count rate, where the solid line is the initial, conditionally ideal probability distribution; dotted line – after adding speckle noise; + – after the smoothing procedure

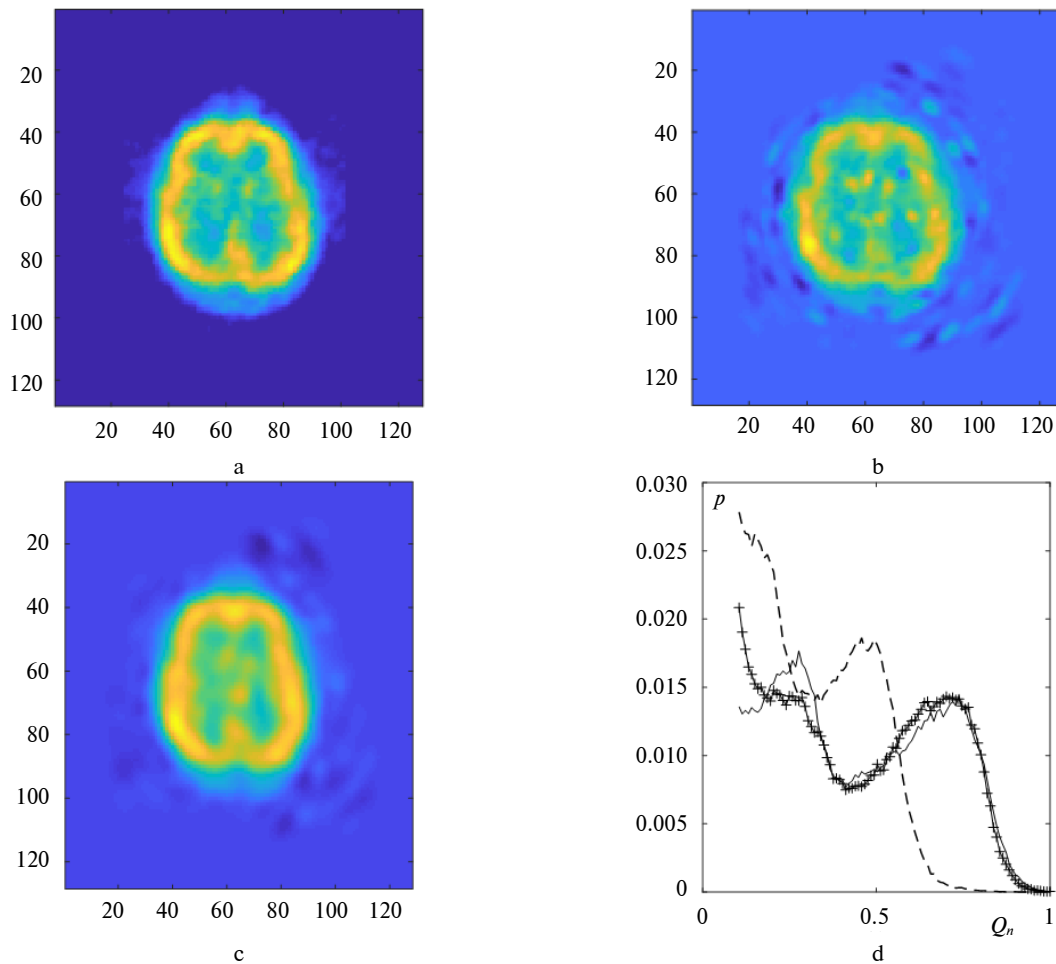


**Figure 8:** An example of the results of smoothing SPECT of a patient's brain in accordance with (2): (a), (b), (c) cross-sections before, after adding speckle noise, and smoothing, respectively; (d) the probability distribution functions of the count rate, where the solid line is the initial, conditionally ideal probability distribution; dotted line – after adding speckle noise; + – after the smoothing procedure

## Discussion

A lot of articles have been published on the optimal filtering of SPECT images [12, 14–24]. The vast majority of publications focus on the use of the Butterworth filter [12, 14–18]. At the same time, it should be noted that it is difficult to single out recommendations for choosing a cutoff frequency. So, in [14] the optimal cutoff frequency is in the range 0.08–0.13, in [16, 25] – 0.2–0.22, in [18] – more than 0.5 depending on the RC speed. The parameters of optimal image filtering based on the Gaussian filter [22, 23, 26] are also contradictory and do not allow our working group to make a decision.

A specific direction in the development of technology for improving the quality of radionuclide brain images is the analysis and processing of multimodal data [27–29]. However, it should be noted that it is not always possible to obtain multimodal images; an increase in image resolution does not mean a more correct restoration of the spatial distribution of the radiopharmaceuticals in absolute units; the corresponding software has not been introduced into wide clinical practice, into workstations of gamma cameras.

The research results presented in this work are solving a specific applied problem: restoration of the histogram of the distribution of radiopharmaceuticals in a brain for a correct quantitative assessment of regional CBF. It is taken into account that the initial 3D tomographic data contain not only uniform random Gaussian noise, but also a pronounced speckle component. The technique has been tested in solving clinical problems, in particular in patients with moderate brain injury due to combat contusion [30].

The presented research results retained their regularities for SPECT of the water phantom with the data acquisition matrix of 256×256. The following limitations can be distinguished for images with a matrix of 64×64 in the analysis of patients' SPECT:  $0.2 \leq \sigma_{f0} \leq 1.5$  and  $n_f = 3$ .

It should also be noted that the technique presented in this work does not give significant positive results with pronounced sparseness of scintigraphic projection images, which are formed with a sharply reduced total CR or with a short exposure time of the frame during the SPECT study. The solution of the applied problem is not trivial and requires further research. This problem is considered, for example, in [31].

A novel technique for smoothing 3D SPECT images based on a Gaussian filter was developed. It was shown that the change in the maximum rate of the SPECT image RC has an extremum by changing

the standard deviation of the Gaussian filter in vicinity of 0.3–0.4 pixels. The greater the noise component in the SPECT image, the more quasi-linearly the corresponding speed changes. This dependence allows us to determine the optimal smoothing parameters.

The application of the developed smoothing technique allows restoring the probability distribution function of the radioactive CR (distribution histogram) with an accuracy of 5–10%. This allows standardizing SPECT images, in particular, of a brain, and carrying out image segmentation more correctly.

## Conclusions

The research results of the work solve a specific applied problem: restoration of the histogram of the radiopharmaceuticals distribution in a brain for correct quantitative assessment of regional cerebral blood flow. In contrast to the well-known publications on the filtration of SPECT data, the work takes into account that the initial tomographic data are 3D, rather than 2D slices, and contain not only uniform random Gaussian noise, but also a pronounced speckle component. This allows standardization of brain SPECT images in terms of the spatial distribution of the radiopharmaceuticals in a brain.

## Acknowledgements

The authors are grateful to the SI "Institute of Neurosurgery named after acad. A.P. Romodanov of the National Academy of Medical Sciences of Ukraine" for the opportunity to perform the work.

**Interests Disclosure:** Nikolay Nikolov, Sergiy Makeyev, Tetyana Novikova, Yelizaveta Kriukova, Olga Korostynska declare that they have no conflict of interest. The work was performed as part of research in SI "Romodanov Neurosurgery Institute of the National Academy of Medical Sciences of Ukraine" (Kyiv, Ukraine); State registration number: 0116U001031 "To investigate the polymodal evoked potentials of the brain, including cognitive, in patients with chronic ischemia in the vertebral-basilar basin, depending on disorders of cerebral blood suppl"; engineering studies were performed on a without payment (by initiative of the authors).

**Informed consent:** Informed consent was obtained from all individual participants included in the study.

**Ethical approval:** All procedures performed in studies involving human participants were carried out in accordance with the Declaration of Helsinki 1964 and its later amendments, the European Convention on Human Rights, which have been ratified

by Ukraine and are an integral part of national legislation.

This article does not contain any animal studies performed by any of the authors.

## References

- [1] Nikolov NA, Makeev SS, Yaroshenko OYu, Novikova TG, Globa MV. Quantitative evaluation of cerebral blood flow by scintigraphic studies with <sup>99m</sup>Tc-HMPAO. *Meditsinskaya Fizika*. 2016;72:72-9.
- [2] Nikolov N, Makeyev S, Yaroshenko O, Novikova T, Globa M. Quantitative evaluation of the absolute value of the cerebral blood flow according to the scintigraphic studies with <sup>99m</sup>Tc-HMPAO. *Res Bull Nat Tech Univ Ukr Kyiv Polytech Inst*. 2017;1:61-8. DOI: 10.20535/1810-0546.2017.1.91646
- [3] Lassen NA, Andersen AR, Friberg L, Paulson OB. The retention of [<sup>99m</sup>Tc]-d,l-HM-PAO in the human brain after intracarotid bolus injection: A kinetic analysis. *J Cereb Blood Flow Metab*. 1988 Dec;8(1\_suppl):S13-22. DOI: 10.1038/jcbfm.1988.28
- [4] Andersen AR, Friberg HH, Schmidt JF, Hasselbalch SG. Quantitative measurements of cerebral blood flow using SPECT and [<sup>99m</sup>Tc]-d,l-HM-PAO compared to Xenon-133. *J Cereb Blood Flow Metab*. 1988 Dec;8(1\_suppl):S69-81. DOI: 10.1038/jcbfm.1988.35
- [5] Nikolov NA, Makeev SS, Novikova TG, Chebotariova LL, Globa MV, Unevich OA, et al. Determination of absolute cerebral blood flow scintigraphy with lipophilic radiopharmaceutical. *Meditsinskaya Fizika*. 2018;79:36-45.
- [6] Saxena P, Pavel DG, Quintana JC, Horwitz B. An automatic threshold-based scaling method for enhancing the usefulness of Tc-HMPAO SPECT in the diagnosis of Alzheimer's disease. In: Wells WM, Colchester A, Delp S, editors. *Medical image computing and computer-assisted intervention – MICCAI'98*. MICCAI 1998. Lecture notes in computer science, vol. 1496. Berlin Heidelberg: Springer; 1998. p. 623-30. DOI: 10.1007/BFb0056248
- [7] Fahey FH, Bom HH, Chiti A, Choi YY, Huang G, Lassmann M, et al. Standardization of administered activities in pediatric nuclear medicine: A report of the first nuclear medicine global initiative project, Part 2—Current standards and the path toward global standardization. *J Nucl Med*. 2016 Jul;57(7):1148-57. DOI: 10.2967/jnumed.115.169714
- [8] Kapucu ÖL, Nobili F, Varrone A, Booi J, Vander Borgh T, Nägren K, et al. EANM procedure guideline for brain perfusion SPECT using <sup>99m</sup>Tc-labelled radiopharmaceuticals, version 2. *Eur J Nucl Med Mol Imaging*. 2009 Dec;36(12):2093-102. DOI: 10.1007/s00259-009-1266-y
- [9] Diaz MP, Rizo OD, Dñaz AL, Aparicio EE, Dñaz RR. Activity optimization method in SPECT: A comparison with ROC analysis. *J Zhejiang Univ Sci B*. 2006 Dec;7(12):947-56. DOI: doi.org/10.1631/jzus.2006.B0947
- [10] Jang MY, Park CR, Kang S, Lee Y. Experimental study of the fast non-local means noise reduction algorithm using the Hoffman 3D brain phantom in nuclear medicine SPECT image. *Optik*. 2020 Dec;224:165440. DOI: 10.1016/j.ijleo.2020.165440
- [11] Modzelewski R, Janvresse E, de la Rue T, Vera P. Comparison of heterogeneity quantification algorithms for brain SPECT perfusion images. *EJNMMI Res*. 2012;2(1):40. DOI: 10.1186/2191-219X-2-40
- [12] Lyra M, Ploussi A. Filtering in SPECT image reconstruction. *Int J Biomed Imaging*. 2011;2011:1-14. DOI: 10.1155/2011/693795
- [13] Bruyant PP. Analytic and iterative reconstruction algorithms in SPECT. *J Nucl Med*. 2002 Oct;43(10):1343-58.
- [14] Minoshima S, Maruno H, Yui N, Togawa T, Kinoshita F, Kubota M, et al. Optimization of Butterworth filter for brain SPECT imaging. *Ann Nucl Med*. 1993 Jun;7(2):71-7. DOI: 10.1007/BF03164571
- [15] Van Laere K, Koole M, Lemahieu I, Dierckx R. Image filtering in single-photon emission computed tomography: principles and applications. *Comput Med Imaging Graph*. 2001 Mar;25(2):127-33. DOI: 10.1016/S0895-6111(00)00063-X
- [16] Liu H-G, Harris JM, Inampudi CS, Mountz JM. Optimal reconstruction filter parameters for multi-headed brain SPECT: Dependence on count activity. *J Nucl Med Technol*. 1995;23:251-7.
- [17] Dong X, Saripan M, Mahmud R, Mashohor S, Wang A. Determination of the optimum filter for <sup>99m</sup>Tc SPECT breast imaging using a wire mesh collimator. *Pak J Nucl Med*. 2017;7(1):9-15. DOI: 10.24911/PJNMed.7.2
- [18] Onishi H, Matsutake S, Amijima H. Validation of optimal cut-off frequency using a Butterworth filter in single photon emission computed tomography reconstruction for the target organ: Spatial domain and frequency domain. *J Faculty of Health and Welfare Prefectural University of Hiroshima*. 2010;10(1): 27-36.
- [19] Sowa-Staszczak A, Lenda-Tracz W, Tomaszuk M, Głowa B, Hubalewska-Dydejczyk A. Optimization of image reconstruction method for SPECT studies performed using [<sup>99m</sup>Tc-EDDA/HYNIC] octreotate in patients with neuroendocrine tumors. *Nucl Med Rev*. 2013 Feb 8;16(1):9-16. DOI: 10.5603/NMR.2013.0003
- [20] King MA, Glick SJ, Penney BC, Schwinger RB, Doherty PW. Interactive visual optimization of SPECT prereconstruction filtering. *J Nucl Med*. 1987;28:1192-8.

- [21] Huang C, Wu J, Cheng K, Pan L. Optimization of imaging parameters for SPECT scans of [<sup>99m</sup>Tc]TRODAT-1 using Taguchi analysis. *PLoS ONE*. 2015 Mar 19;10(3):e0113817. DOI: 10.1371/journal.pone.0113817
- [22] Beekman FJ, Slijpen ETP, Niessen WJ. Supervised diffusion parameter selection for filtering SPECT brain images. In: ter Haar Romeny B, Florack L, Koenderink J, Viergever M, editors. *Scale-space theory in computer vision. Scale-space 1997. Lecture notes in computer science*, vol. 1252. Berlin, Heidelberg: Springer; 1997. p. 164–75. DOI: 10.1007/3-540-63167-4\_48
- [23] Razifar P, Sandström M, Schnieder H, Långström B, Maripuu E, Bengtsson E, et al. Noise correlation in PET, CT, SPECT and PET/CT data evaluated using autocorrelation function: a phantom study on data, reconstructed using FBP and OSEM. *BMC Med Imaging*. 2005 Dec;5(1):5–23. DOI: 10.1186/1471-2342-5-5
- [24] Brambilla M, Cannillo B, Dominietto M, Leva L, Secco C, Inglese E. Characterization of ordered-subsets expectation maximization with 3d post-reconstruction gauss filtering and comparison with filtered backprojection in <sup>99m</sup>Tc SPECT. *Ann Nucl Med*. 2005 Apr;19(2):75–82. DOI: 10.1007/BF03027384
- [25] Morano GN, Seibyl JP. Technical overview of brain SPECT imaging: improving acquisition and processing of data. *J Nucl Med Technol*. 2003 Dec;31(4):191–5; quiz 202–3.
- [26] Beekman FJ, Slijpen ETP, Niessen WJ. Selection of task-dependent diffusion filters for the post-processing of SPECT images. *Phys Med Biol*. 1998 Jun 1;43(6):1713–30. DOI: 10.1088/0031-9155/43/6/024
- [27] Vija AH, Cachovan M. Multi-modal reconstruction in brain perfusion SPECT. *J Nucl Med*. 2019;60 (supplement 1):1362.
- [28] Li T, Wang Y. Multiscaled combination of MR and SPECT images in neuroimaging: A simplex method based variable-weight fusion. *Comput Methods Programs Biomed*. 2012 Jan;105(1):31–9. DOI: 10.1016/j.cmpb.2010.07.012
- [29] Liu Z, Song Y, Sheng VS, Xu C, Maere C, Xue K, et al. MRI and PET image fusion using the nonparametric density model and the theory of variable-weight. *Comput Methods Programs Biomed*. 2019 Jul;175:73–82. DOI: 10.1016/j.cmpb.2019.04.010
- [30] Novikova T, Nikolov N, Makeev S, Steblyuk V. SPECT in the diagnosis of cerebral changes in patients in the intermediate and long-term periods of combat explosive mild traumatic brain injury. *Eurasian J Oncol*. 2020;8(3):260–70. Available from: [https://onco.recipe.by/en/?editions=2020-tom-8-n-3&group\\_id=item\\_0&article\\_id=line\\_3](https://onco.recipe.by/en/?editions=2020-tom-8-n-3&group_id=item_0&article_id=line_3)
- [31] Zheng W, Li S, Krol A, Ross Schmidlein C, Zeng X, Xu Y. Sparsity promoting regularization for effective noise suppression in SPECT image reconstruction. *Inverse Problems*. 2019 Nov 1;35(11):115011. DOI: 10.1088/1361-6420/ab23da

М.О. Ніколов<sup>1,4</sup>, С.С. Макеєв<sup>2</sup>, О. Коростинська<sup>3</sup>, Т.Г. Новікова<sup>2</sup>, Є.С. Крюкова<sup>1</sup>

<sup>1</sup>КПІ ім. Ігоря Сікорського, Київ, Україна

<sup>2</sup>ДУ “Інститут нейрохірургії ім. акад. А.П. Ромоданова НАМН України”, Київ, Україна

<sup>3</sup>Столичний університет Осло, Осло, Норвегія

<sup>4</sup>ДУ “Інститут медицини праці імені Ю.І. Кундієва НАМН України”, Київ, Україна

#### ФІЛЬТР ГАУСА ДЛЯ ОФЕКТ-ЗОБРАЖЕНЬ ГОЛОВНОГО МОЗКУ

**Проблематика.** Наявність шумової складової на 3D-зображеннях однофотонної емісійної комп’ютерної томографії (ОФЕКТ) головного мозку суттєво спотворює функцію розподілу ймовірностей (ФРЙ) швидкості радіоактивного рахунку. Наявність шумів і подальша фільтрація даних, що базується на суб’єктивній оцінці якості зображень, значно впливають на розрахунок об’ємного мозкового кровотоку та значення асиметрії накопичення радіофармпрепарату в мозку.

**Мета.** Розробка методу оптимальної ОФЕКТ-фільтрації зображень головного мозку з ліпофільними радіофармпрепаратами на основі фільтра Гауса (ГФ) для подальшої сегментації зображень пороговим методом.

**Методика реалізації.** В роботі аналізувалися ОФЕКТ-зображення водного фантому та головного мозку пацієнтів з <sup>99m</sup>Tc-ГМПАО. Розроблено методику штучного додавання спекл-шуму до умовно ідеальних даних для визначення оптимальних параметрів згладжування ОФЕКТ на основі ФГ. Кількісним критерієм оптимального згладжування слугувало середньоквадратичне відхилення між ФРЙ швидкості радіоактивного рахунку між згладженими зображеннями та умовно ідеальним.

**Результати.** Показано, що максимальна швидкість радіоактивного рахунку ОФЕКТ-зображення має екстремум при зміні стандартного відхилення ГФ за просторового порядку фільтра в діапазоні 0,3–0,4 пікселя. Чим більша шумова складова на зображеннях ОФЕКТ, тим більш квазілінійно змінюється відповідна швидкість. Ця залежність дає змогу визначити оптимальні параметри згладжування. Застосування розробленої методики згладжування дає можливість відновити функцію розподілу ймовірностей швидкості радіоактивного рахунку (гістограма розподілу) з точністю до 5–10 %. Це дає змогу стандартизувати ОФЕКТ-зображення головного мозку з точки зору просторового розподілу препарату в мозку.

**Висновки.** Представлені в роботі результати досліджень вирішують конкретне завдання – відновлення гістограми розподілу радіофармпрепаратів в мозку для коректної кількісної оцінки об’ємного мозкового кровотоку. На відміну від відомих публікацій про фільтрацію даних ОФЕКТ, у роботі враховується, що вихідні томографічні дані є 3D, а не представлені 2D-зрізами, і містять не тільки рівномірний випадковий гаусівський шум, але й виражену спекл-складову.

**Ключові слова:** емісійна комп’ютерна томографія; ОФЕКТ; мозковий кровоток; радіоактивний рахунок; фільтр Гауса; оптимальна фільтрація; радіофармпрепарати; <sup>99m</sup>Tc-ГМПАО.

Н.А. Николов<sup>1,4</sup>, С.С. Макеев<sup>2</sup>, О. Коростинская<sup>3</sup>, Т.Г. Новикова<sup>2</sup>, Е.С. Крюкова<sup>1</sup>

<sup>1</sup>КПИ им. Игоя Сикорского, Киев, Украина

<sup>2</sup>ГУ "Институт нейрохирургии им. акад. А. П. Ромоданова НАМН Украины", Киев, Украина

<sup>3</sup>Столичный университет Осло, Осло, Норвегия

<sup>4</sup>ГУ "Институт медицины труда имени Ю.И. Кундиева НАМН Украины", Киев, Украина

### ФИЛЬТР ГАУССА ДЛЯ ОФЭКТ-ИЗОБРАЖЕНИЙ ГОЛОВНОГО МОЗГА

**Проблематика.** Наличие шумовой составляющей на 3D-изображениях однофотонной эмиссионной компьютерной томографии (ОФЭКТ) головного мозга существенно искажает функцию распределения вероятностей (ФРВ) скорости радиоактивного счета. Наличие шумов и последующая фильтрация данных, основанная на субъективной оценке качества изображений, оказывают значительное влияние на расчет объемного мозгового кровотока и значения асимметрии накопления радиофармпрепарата в мозге.

**Цель.** Разработка метода оптимальной ОФЭКТ-фильтрации изображений головного мозга с липофильными радифармпрепаратами на основе фильтра Гаусса (ГФ) для последующей сегментации изображения пороговым методом.

**Методика реализации.** В работе анализировались ОФЭКТ-изображения водного фантома и головного мозга пациентов с <sup>99m</sup>Tc-ГМПАО. Разработана методика искусственного добавления спекл-шума к условно идеальным данным для определения оптимальных параметров сглаживания ОФЭКТ на основе ФГ. Количественным критерием оптимального сглаживания служило среднеквадратичное отклонение между ФРВ скорости радиоактивного счета между сглаженными изображениями и условно идеальным.

**Результаты.** Показано, что максимальная скорость радиоактивного счета ОФЭКТ-изображения имеет экстремум при изменении стандартного отклонения ГФ для пространственного порядка фильтра в диапазоне 0,3–0,4 пикселя. Чем больше шумовая составляющая на изображениях ОФЭКТ, тем более квазилинейно изменяется соответствующая скорость. Эта зависимость позволяет определить оптимальные параметры сглаживания. Применение разработанной методики сглаживания позволяет восстановить функцию распределения вероятностей скорости радиоактивного счета (гистограмму распределения) с точностью до 5–10 %. Это позволяет стандартизировать ОФЭКТ-изображения головного мозга с точки зрения пространственного распределения препарата в мозге.

**Выводы.** Представленные в данной работе результаты исследований решают конкретную прикладную задачу – восстановление гистограммы распределения радиофармпрепаратов в мозге для корректной количественной оценки объемного мозгового кровотока. В отличие от известных публикаций про фильтрацию данных ОФЭКТ, в работе учитывается, что исходные томографические данные являются 3D, а не представлены 2D-срезами, и содержат не только равномерный случайный гауссовский шум, но и выраженную спекл-составляющую.

**Ключевые слова:** эмиссионная компьютерная томография; ОФЭКТ; мозговой кровоток; радиоактивный счет; фильтр Гаусса; оптимальная фильтрация; радифармпрепараты; <sup>99m</sup>Tc-ГМПАО.